

LJMU Research Online

Fergus, P, Selvaraj, M and Chalmers, C

Machine learning Ensemble Modelling to classify caesarean section and vaginal delivery types using cardiotocography traces

<http://researchonline.ljmu.ac.uk/id/eprint/7696/>

Article

Citation (please note it is advisable to refer to the publisher's version if you intend to cite from this work)

Fergus, P, Selvaraj, M and Chalmers, C (2017) Machine learning Ensemble Modelling to classify caesarean section and vaginal delivery types using cardiotocography traces. Computers in Biology and Medicine, 93 (1). pp. 7-16. ISSN 0010-4825

LJMU has developed **LJMU Research Online** for users to access the research output of the University more effectively. Copyright © and Moral Rights for the papers on this site are retained by the individual authors and/or other copyright owners. Users may download and/or print one copy of any article(s) in LJMU Research Online to facilitate their private study or for non-commercial research. You may not engage in further distribution of the material or use it for any profit-making activities or any commercial gain.

The version presented here may differ from the published version or from the version of the record. Please see the repository URL above for details on accessing the published version and note that access may require a subscription.

For more information please contact researchonline@ljmu.ac.uk

Machine Learning Ensemble Modelling to Classify Caesarean Section and Vaginal Delivery Types Using Cardiotocography Traces

Paul Fergus, Selvaraj Malarvizhi, and Carl Chalmers

*Liverpool John Moores University,
Faculty of Engineering and Technology,
Data Science Research Centre,
Department of Computer Science,
Byron Street,
Liverpool,
L3 3AF,
United Kingdom.*

Machine Learning Ensemble Modelling to Classify Caesarean Section and Vaginal Delivery Types Using Cardiotocography Traces

ABSTRACT

Human visual inspection of Cardiotocography traces is used to monitor the foetus during labour and avoid neonatal mortality and morbidity. The problem, however, is that visual interpretation of Cardiotocography traces is subject to high inter and intra observer variability. Incorrect decisions, caused by miss-interpretation, can lead to adverse perinatal outcomes and in severe cases death. This study presents a review of human Cardiotocography trace interpretation and argues that machine learning, used as a decision support system by obstetricians and midwives, may provide an objective measure alongside normal practices. This will help to increase predictive capacity and reduce negative outcomes. A robust methodology is presented for feature set engineering using an open database comprising 552 intrapartum recordings. State-of-the-art in signal processing techniques is applied to raw Cardiotocography foetal heart rate traces to extract 13 features. Those with low discriminative capacity are removed using Recursive Feature Elimination. The dataset is imbalanced with significant differences between the prior probabilities of both normal deliveries and those delivered by caesarean section. This issue is addressed by oversampling the training instances using a synthetic minority oversampling technique to provide a balanced class distribution. Several simple, yet powerful, machine-learning algorithms are trained, using the feature set, and their performance is evaluated with real test data. The results are encouraging using an ensemble classifier comprising Fishers Linear Discriminant Analysis, Random Forest and Support Vector Machine classifiers, with 87% (95% Confidence Interval: 86%, 88%) for Sensitivity, 90% (95% CI: 89%, 91%) for Specificity, and 96% (95% CI: 96%, 97%) for the Area Under the Curve, with a 9% (95% CI: 9%, 10%) Mean Square Error.

Keywords: *Perinatal Complications, Cardiotocography, Classification, Data Science, Machine Learning, Ensemble Modelling*

1. INTRODUCTION

UNICEF estimates that 130 million babies are born each year. One million of these will be intrapartum stillbirths and more than three and a half million will die as a result of perinatal complications [1]. The number of reported deliveries in the UK during 2012 was 671,255. One in every 200 resulted in stillbirth and 300 died in the first four weeks of life [2]. Between one and seven in every 1000 foetuses experienced hypoxia (impaired delivery of oxygen to the brain and tissue) [3] that resulted in adverse perinatal outcomes and in severe cases death [4]. During 2013, according to Tommy's charity, the rate of stillbirths in the UK was 4.7 per 1000 births. In 2014, 1,300 babies were injured at birth due to mistakes made by maternity staff, which cost the National Health Service (NHS) in the UK more than £1 billion in compensation and more than £500 million in legal fees to resolve disputes.

Human visual pattern recognition in Cardiotocography (CTG) traces is used to monitor the foetus during the early stages of delivery [5]. CTG devices, fitted to the abdomen, record the foetal heartbeat and uterine contractions [6]. The foetal heart rate recordings represent the modulation influence provided by the central nervous system. When the foetus is deprived of oxygen, the cardiac function is impaired. Detecting its occurrence can be confirmed by cord blood (umbilical artery) metabolic acidosis with a base deficit of more than 15mmol/L [7]. The etiology is not clear however, environmental factors, such as umbilical cord compression and maternal smoking, are known risk factors [8].

Obstetricians and midwives use CTG traces to formulate clinical decisions. However, poor human interpretation of traces and high inter and intra observer variability, [9]–[11] makes the prediction of neonatal outcomes challenging. CTG was introduced into clinical practice 45 years ago. Since then there has been no significant evidence to suggest its use has improved the rate of perinatal deaths. However, several studies do argue that 50% of birth-related brain injuries could have been prevented if CTG was interpreted correctly [12]. Conversely, there is evidence to indicate that over-interpretation increases the number of births delivered by caesarean section even when there are no known risk factors [13].

Computerised CTG has played a significant role in developing objective measures as a function of CTG signals [14], particularly within the machine learning community [15]–[18], [7],[12], [19]–[23]. According to a Cochrane report in 2015, computerised interpretation of CTG traces significantly reduced perinatal mortality [24]. In this study, we build on previous works and utilise an open dataset obtained from Physionet. The dataset contains CTG trace recordings for normal vaginal births (506) and those that were delivered by caesarean section (46). Several machine-learning algorithms are trained using features extracted from raw CTG Foetal Heart Rate (FHR) traces contained in the dataset to distinguish between caesarean section and vaginal delivery types. This would allow for the optimisation of decision making, by obstetricians and midwives, in the presence of FHR traces, linked to caesarean section and normal vaginal deliveries. The results demonstrate that an ensemble classifier produces better results than several studies reported in the literature.

2. ANALYSIS

2.1 Cardiotocography Feature Extraction

Feature extraction techniques are used to gather specific parameters from a signal. These are often more efficient to analyse than the raw signal samples themselves. Signal processing does not increase the information content but rather incurs information loss caused by feature extraction. However, this is preferable to raw data analysis, as it simplifies classification tasks. The features extracted can be broadly divided into two groups, linear and nonlinear. In both of these groups, all signal data points are transformed (using a linear or nonlinear transformation) into a reduced dimensional space. Thus, the original data points are replaced with a smaller set of discriminative variables. For a more detailed discussion on feature extraction please refer to [25].

Linear features can be broadly defined as those features that are visible through human inspection, for example accelerations and decelerations in the foetal heartbeat. While, nonlinear features are much more difficult to interpret or even identify under normal visual analysis. For example, formally quantifying the complexity of a signal and the differences between two or more observations is practically impossible to achieve through visual inspection alone.

The International Federation of Gynaecology and Obstetrics (FIGO) and the National Institute for Health and Care Excellence (NICE) in the UK have developed guidelines used to interpret CTG traces [26]. These are briefly described in Table 1.

Feature	Baseline (bpm)	Variability (bpm)	Decelerations	Accelerations
Reassuring	110-160	≥ 5	None	Present
Non-Reassuring	100-109 161-180	<5 for 40-90 minutes	Typical variable decelerations with over 50% of contractions, occurring for over 90 minutes. Single prolonged deceleration for up to 3 minutes	The absence of accelerations with otherwise normal trace is of uncertain significance
Abnormal	<100 >180 Sinusoidal pattern ≥ 10 minutes	<5 for 90 minutes	Either typical variable decelerations with over 50% of contractions or late decelerations, both for over 30 minutes. Single prolonged deceleration for more than 3 minutes	

Table 1 - Classification of FHR Trace Features (Baseline, Variability, Decelerations and Accelerations)

The FIGO features include the real FHR baseline (RBL), Accelerations, Decelerations, Short-Term variability (STV) and Long-Term variability (LTV). To understand how the RBL is obtained (and used to derive all other features) consider Figure 1. The RBL is calculated as the mean of the signal [27] with the peaks and troughs removed (signals that reside outside the baseline min and max thresholds). Peaks and troughs are removed using a virtual baseline (VBL) which is the mean of the complete signal (with peaks a troughs) and the removal of signals that are ± 10 bpm from the VBL.

Acceleration and Deceleration coefficients are obtained by counting the number of transient increases and decreases from the RBL, that are ± 10 bpm and last for 10s or more [28]. Accelerations typically indicate adequate blood delivery and are reassuring for medical practitioners. While decelerations result from physiological provocation (i.e. compromised oxygenation resulting from uterine contractions). If Decelerations do not recover (the absence of Accelerations), this can indicate the presence of umbilical cord compression, foetal hypoxia or metabolic acidosis [29].

Meanwhile, STV is calculated as the average of 2.5-second blocks in the signal averaged over the duration of the signal. LTV, on the other hand, describes the difference between the minimum and maximum value in a 60-second block averaged over the duration of the signal. The presence of both STV and LTV describe normal cardiac function [30]. If STV or LTV decreases or is absent, this could indicate the onset of an adverse pathological outcome [31].

FIGO features represent the morphological structure of the FHR signal and are the visual cues used by obstetricians and midwives to monitor the foetus. However, using these alone has seen high inter and intra variability. This has led to studies designed to extract non-linear features (not easily identifiable through human visual inspection) from the FHR signal to try to improve and support outcome measures obtained by obstetricians and midwives [32].

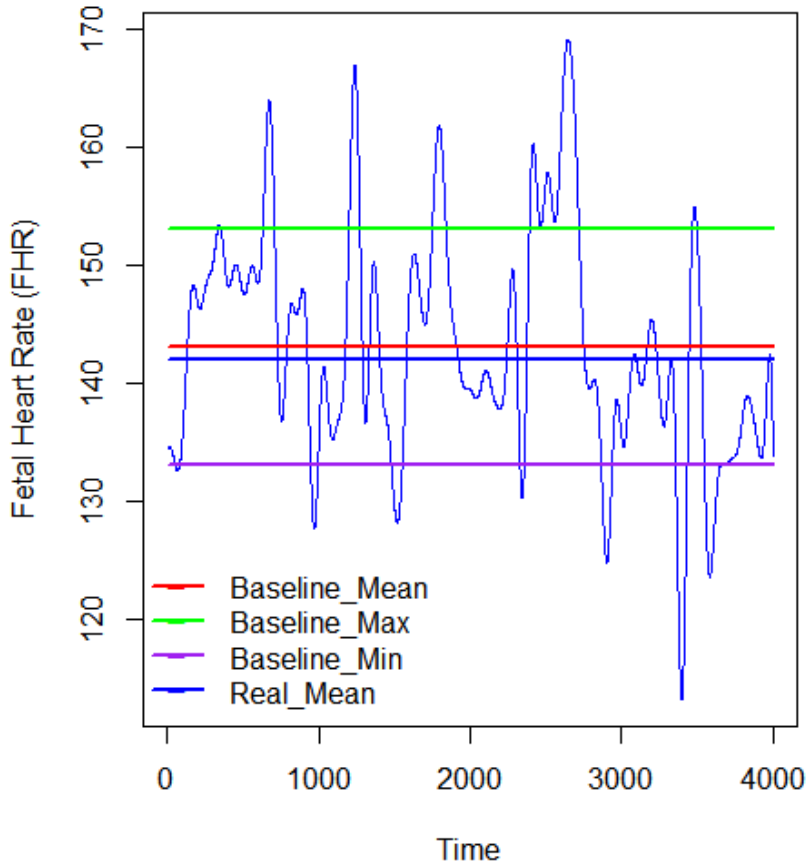


Figure 1: Using the FHR signal (Beats per Minute) to calculate the Real Baseline

Root Mean Squares (RMS) and Sample Entropy (SampEn) are two signal processing coefficients that are commonly used in antepartum and intrapartum studies to represent the non-visual patterns contained in the FHR [33]–[36]. RMS measures the magnitude of the varying quantity and is an effective signal strength indicator in heart rate variability studies. Sample entropy on the other hand represents the non-linear dynamics and loss of complexity in the FHR, and is a useful indicator for foetal hypoxia and metabolic-acidosis detection [37].

CTG signals are also translated into frequency representations, via Fast Fourier Transform (FFT) [38] and Power Spectral Density (PSD) to minimise signal quality variations [39]. In the context of FHR analysis, frequency features have been successfully used in [40] and more recently in [41] and [42]. For example, Peak Frequency (FPeak) is derived from the PSD and used in antepartum and intrapartum analysis to measure variability and normal sympathetic and parasympathetic function [33], [34], [43].

Meanwhile, non-linear features [44], such as Poincare plots, have seen widespread use in heart rate variability studies [45]. In this study, the difference between two beats (BB) is calculated rather than the normal RR interval used in PQRST analysis. The two descriptors of the plot are SD1 and SD2. These coefficients are associated with the standard deviation of BB and the standard deviation of the successive difference of the BB interval. The ratio of SD1/SD2 (SDRatio) describes the relation between short and long-term variations of BB.

The box-counting dimension (FD) enables the dynamics of the FHR to be estimated [46] and is a direct measure of the morphological properties of a signal. The signal is covered with

optimally sized boxes where the number of boxes describes the box-counting dimension coefficient. In previous studies, these features have proven to be an effective indicator for foetal hypoxia and metabolic acidosis detection [47].

In the case of self-affinity measures in FHR signals, previous studies have demonstrated that it is a beneficial coefficient in classification tasks [48]. Detrend Fluctuation Analysis (DFA) produces an exponent value that indicates the presence or absence of self-similarity [49]. DFA examines the signal at different time scales and returns a fractal scaling exponent x . The calculations are repeated for all considered window sizes defined as n . In this instance, the focus is on the relation between $F(n)$ and the size of the window n . In general, $F(n)$ will increase with the size of window n .

2.2 Automated Cardiotocography Classification

Computer algorithms are utilised extensively in biomedical research and are a fundamental component within most clinical decision support systems. CTG is no different, where machine learning algorithms have proven to be excellent decision makers in CTG analysis.

For example, Warrick *et al.* [15] developed a system to model FHR and Uterine Contraction (UC) signal pairs to estimate their dynamic relation [50]. The authors conclude that it is possible to detect approximately half of the pathological cases one hour and 40 minutes before delivery with a 7.5% false positive rate. Kessler *et al.* [54] on the other hand applied CTG and ST waveform analysis resulting in timely intervention for caesarean section and vaginal deliveries [7].

In a similar study, Blinx *et al.* [51] compared a Decision Tree (DT), an Artificial Neural Network (ANN), and Discriminant Analysis (DA). The ANN classifier obtain 97.78% overall accuracy. The *Sensitivity* and *Specificity* values were not provided making accuracy alone an insufficient performance measure. Ocak *et al.* [52] evaluated an SVM and Genetic Algorithm (GA) classifier and reported 99.3% and 100% accuracies for normal and pathological delivery outcomes. Similar results were reported in [53] and [54]. Again, *Sensitivity* and *Specificity* values were not provided. Meanwhile Menai *et al* [55] classified foetal state using a Naive Bayes (NB) classifier with four different feature selection (FS) techniques: Mutual Information, Correlation-based, ReliefF, and Information Gain. The NB classifier in conjunction with ReliefF features produced 93.97%, 91.58%, and 95.79% for *Accuracy*, *Sensitivity* and *Specificity*, respectively.

While, Karabulut *et al.* [56] utilised an adaptive boosting (AdaBoost) classifier producing an accuracy of 95.01% - again no *Sensitivity* or *Specificity* values were provided. While Spilka *et al.*, [13], used a Random Forest (RF) classifier and latent class analysis (LCA) [57] producing *Sensitivity* and *Specificity* values of 72% and 78% respectively [5]. Generating slightly better results in [45], Spilka *et al.* attempted to detect perinatal outcomes using a C4.5 decision tree, Naive Bayes, and SVM. The SVM produced the best results using a 10-fold cross validation method, which achieved 73.4% for *Sensitivity* and 76.3% of *Specificity*.

3. METHODOLOGY

In this study all experiments were run on a Dell XPS 13 Developer Edition laptop, with a 6th Gen Intel Core processor and 16GB of memory on Ubuntu version 16.04 LTS. The software developed uses R and RStudio. The data was obtained from Physionet using RDSSamp. Several packages from the CRAN repository are utilised in this study and include the Signal package to filter the FHR signal and the following packages to support the feature extraction process; fractaldim; fractal; pracma; psd; seewave and car. Finally, for the classification and

evaluation tasks the following packages were utilised; MASS, hmeasure, pROC, ROCR randomForest, caret, e1071, and DMwR.

3.1 Dataset Description

Intrapartum recordings were collected between April 2010 and August 2012 from the University Hospital in Brno in Czech Republic (UHB) with the support of the Czech Technical University (CTU) in Prague [5]. The CTG-UHB database is publically available at Physionet. The database contains 552 CTG recordings for singleton pregnancies with a gestational age greater than 36 weeks. The STAN S21/S31 and Avalon FM 40/50 foetal monitors were used to acquire the CTG records. The records do not contain prior known development factors; the duration of stage two labour is less than or equal to 30 minutes; foetal heart rate signal quality is greater than 50 percent in each 30 minute window; and the pH umbilical arterial blood sample is available for each record. 46 records are for deliveries by caesarean section due to pH ≤ 7.20 – acidosis, n=18; pH > 7.20 and pH < 7.25 – foetal deterioration, n=4; and n=24 due to clinical decision without evidence of pathological outcomes) – the remaining 506 records are normal vaginal deliveries. Each record begins no more than 90 minutes before delivery and contains FHR (measured in beats per minute) and UC (measured in mmHg) time series signals – each sampled at 4Hz. The FHR was obtained from an ultrasound transducer attached to the abdominal wall (cardio). The UC was obtained from a pressure transducer also attached to the maternal abdomen (toco). The FHR signal is only considered in this study as it provides direct information about the foetal state. Table 2 summarises the associated clinical data for all records contained in the CTG-UHB database. For a full description of the dataset, please refer to [5].

Table 2: Clinical CTU-UHB Data Summary for Vaginal and Caesarean Section Delivery Types

506 – Vaginal; 46 – Caesarean Section			
	Mean	Min	Max
Maternal Age (Years)	29.8	18	46
Parity	0.43	0	7
Gravidity	1.43	1	11
Gestational Age (Weeks)	40	37	43
pH	7.23	6.85	7.47
BE	-6.36	-26.8	-0.2
BDecf (mmol/l)	4.60	-3.40	26.11
Apgar (1 Minute)	8.26	1	10
Apgar (5 Minute)	9.06	4	10
Length of Stage II. (min)	11.87	0	30
Neonate's Weight (grams)	3408	1970	4750
Neonate's Sex (Male/Female)	293 Male / 259 Female		

Table 3 provides details of the outcome measures used in the CTU-UHB database. For the 46 caesarean section records, the ID is the file number in the CTU-UHB dataset; Age describes the mothers age; pH describes the umbilical artery pH value for each case; BDef is base deficit in extracellular fluid; pCO2 describes the partial pressure of carbon dioxide; BE is base excess; and Apgar scores are a subjective evaluation of the delivery. For a more in-depth discussion of the dataset and these parameters please refer to [5].

Table 3: Caesarean Section Outcome Measures for pH, BDef, pCO2, BE, Apgar1 and Apgar5

ID	Age	pH	BDef	pCO2	BE	Apgar1	Apgar5
2001	30	7.03	22.52	2.8	-23.7	10	10
2002	39	7.27	3.75	6.5	-4.5	7	4
2003	25	6.96	16.96	7.2	-19	6	8
2004	34	6.95	11.44	11.6	-15.3	6	8
2005	31	7.25	3.47	7	-5.5	10	10
2006	32	7.29	NaN	NaN	NaN	10	10
2007	27	7.04	20.42	3.8	-21.8	10	10
2008	26	6.98	13.43	9.3	-16.7	5	7
2009	21	6.96	20.34	5.4	-23	10	10
2010	19	7.3	-0.48	7.2	-1.5	10	10
2011	37	7.01	12.1	9.2	-14.8	3	7
2012	26	7.29	-0.44	7.4	-1.4	9	9
2013	27	6.85	22.63	6.4	-25.3	8	8
2014	34	7.32	2.28	6	-3.2	10	10
2015	29	7.33	4.15	5.3	-5.1	9	10
2016	38	7.27	1.88	7.1	-3.8	9	10
2017	34	7.32	-0.16	6.7	-2	10	10
2018	30	7.31	3.93	5.7	-5	10	10
2019	31	7.29	4.13	6	-5.6	9	9
2020	28	7.15	3.09	9.6	-5.8	4	7
2021	28	7.3	0.19	7	-2.2	9	10
2022	31	7.28	-0.38	7.6	-1.6	9	10
2023	28	6.98	14.49	8.7	-17.4	6	8
2024	39	7.01	7.14	12.1	-10.9	2	4
2025	29	6.99	12.61	9.5	-16	8	8
2026	32	7.23	-0.13	8.7	-2.1	10	10
2027	26	7.31	1.88	6.3	-3.2	9	10
2028	36	7.18	4.82	8.1	-7.2	8	9
2029	34	7.28	1.22	7.1	-3.4	10	10
2030	42	7.04	26.11	0.7	-26.8	10	10
2031	26	7.29	1.52	6.8	-2.9	9	9
2032	35	7.26	3.14	6.9	-4.7	9	10
2033	26	7.39	0.86	5.2	-1.5	9	9
2034	34	7.34	NaN	NaN	NaN	9	9
2035	27	7.26	2.23	7.2	-4.3	8	9
2036	34	7.29	2.5	6.5	-3.7	5	7

2037	29	7.25	1.09	7.8	-3	9	10
2038	27	7.36	3.5	5	-4	5	8
2039	29	7.32	-0.51	6.8	-0.5	9	10
2040	23	7.23	5.27	6.8	-7	2	6
2041	32	7.37	3.69	4.8	-3.1	9	9
2042	27	7.33	-0.5	6.6	-0.8	9	10
2043	26	7.08	10.92	7.9	-13.3	8	9
2044	27	7.02	9.13	10.6	-12.3	8	8
2045	32	7.03	8.91	10.4	-12.2	7	9
2046	19	7.01	NaN	NaN	NaN	5	7

3.2 Signal Pre-processing

The FHR signal contains noise and unwanted artefacts resulting from subjects themselves, the equipment, and the environment [58]. Based on the findings in [59] and [12], the FHR manifests itself predominantly in low frequencies. In [37], [60]–[62] several frequency bands are defined: very low frequency (VLF) at 0-0.03Hz, low frequency (LF) at 0.03-0.15Hz, movement frequency (MF) at 0.15-0.50Hz, and high frequency (HF) at 0.50-1Hz. LF is mainly associated with the activity generated by the sympathetic system, HF with the parasympathetic system, and the MF band with foetal movement and maternal breathing. Both LF and HF frequencies are used in [63] with LF at 0.05-0.2Hz and HF at 0.2-1Hz. However, according to Warrick *et al.* [59], FHR variability at frequencies greater than 0.03Hz are likely noise because there is no power in the FHR signal above this frequency.

In this paper, each of the 552 FHR signal recordings are filtered using a Finite Impulse Response (FIR) 6th order high pass filter with a cut-off frequency of 0.03Hz in accordance with [59]. This was achieved using the R Signal package in RStudio. Phase distortion, introduced by a one-pass filter, is corrected using a two-pass filter. Cubic Hermite spline interpolation is used to remove noise and low-quality artefacts.

3.3 Features Selection

The feature vectors in this study include RBL, Accelerations, Decelerations, STV, LTV, SampEn, FD, DFA, FPeak, RMS, SD1, SD2 and SDRatio. There is general agreement among experts that FIGO features, such as Accelerations and Decelerations, can effectively discriminate between pathological and normal records [64]. However, Spilka *et. al* [45] argue that non-linear features, such as FD and SampEn, have much better discriminative capacity when classifying normal and pathological records, reporting 70% for *Sensitivity*, 78% for *Specificity* and 75% for the Area Under the Curve (*AUC*) using an SVM classifier.

To verify these findings the discriminant capabilities for each feature is determined in this study using a Recursive Feature Elimination algorithm (RFE) [65]. The complete feature set is initially modelled using an RFE algorithm. RFE implements a backwards selection of features based on feature importance ranking. The less important features are sequentially eliminated prior to modelling. The goal is to find a subset of features that can be used to produce an accurate model. Figure 2 highlights the accuracy (cross-validation results) using different feature combinations.

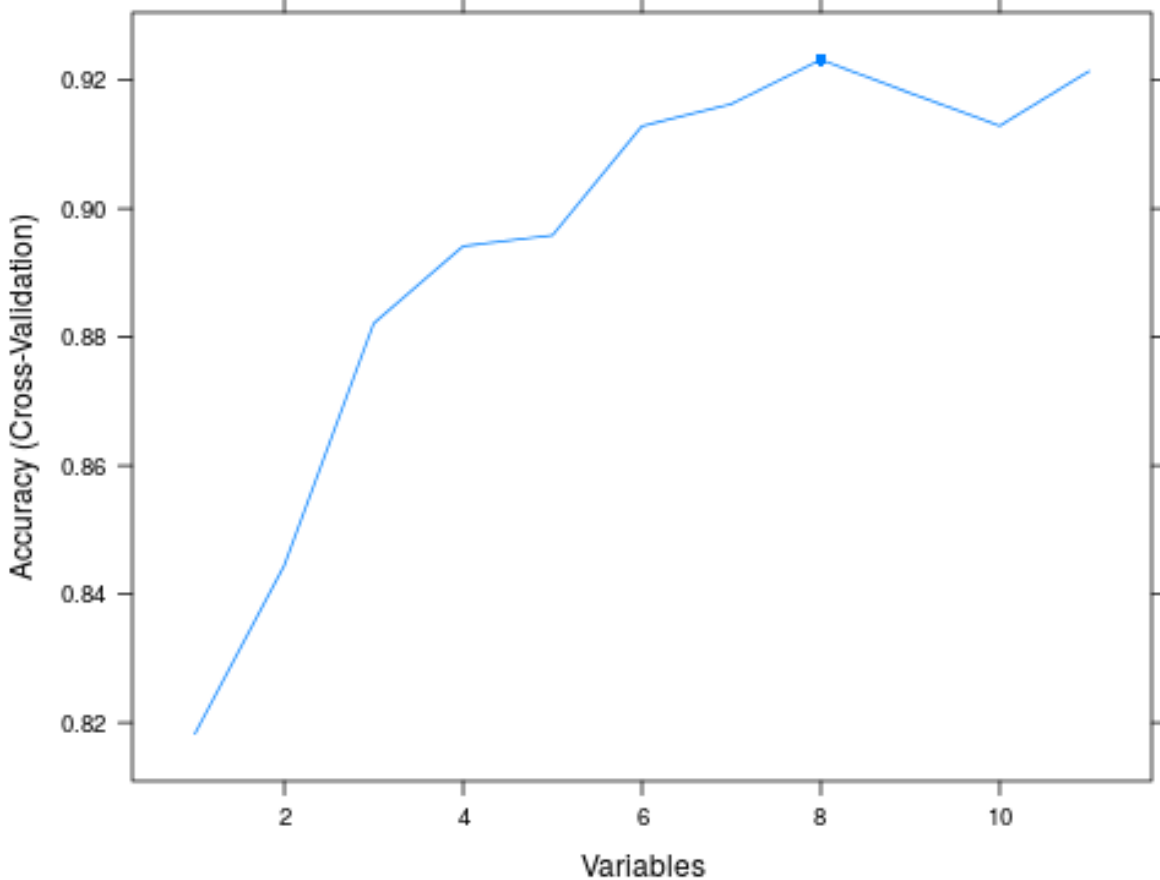


Figure 2: Recursive Feature Elimination using an Accuracy (Cross-Validation) Measure of Importance

The results indicate that it is possible to obtain high accuracies with good Kappa agreement using just eight of the thirteen features as illustrated in Table 3.

Table 3: RFE Feature (Variables) Rankings Using Accuracy and Kappa Estimates

Variables	Accuracy	Kappa	AccSD	KapSD
1	0.8183	0.6384	0.0813	0.1628
2	0.8448	0.6890	0.0345	0.0693
3	0.8821	0.7630	0.0343	0.0685
4	0.8942	0.7861	0.0316	0.0640
5	0.8959	0.7891	0.0370	0.0752
6	0.9129	0.8237	0.0373	0.0755
7	0.9163	0.8305	0.0325	0.0662
8	0.9232	0.8444	0.0377	0.0766
9	0.9180	0.8336	0.0393	0.0798
10	0.9129	0.8231	0.0406	0.0825

11	0.9214	0.8402	0.0354	0.0721
----	--------	--------	--------	--------

The eight ranked features (Variables = eight in Table 3) are DFA, RMS, FD, SD1, SDRatio, SD2, SampEn, and STV. Based on the CTU-UHB dataset, the results support the findings made by Spilka *et al.* [45] that non-linear features, such as DFA, SD1, SD2, and SampEn, have good discriminatory capabilities. Interestingly, the RFE did not rank any of the FIGO-based features with the exception of STV.

3.4 Synthetic minority over-sampling

The CTU-UHB dataset is imbalanced in favour of normal vaginal deliveries (506 normal delivery records and 46 caesarean section cases). Consequently, imbalanced datasets introduce bias during the training phase [1]. Therefore, the probability of classifying a normal vaginal delivery using a random sample will be 91.6% (506/552) compared with classifying a caesarean section delivery, which will be 8.3% (46/552). Consequently, the cost of predicting a term pregnancy that results in a serious pathological outcome is much higher than predicting a caesarean section delivery to find there is no pathological evidence to support the intervention. In this study, this problem is addressed by oversampling the minority class using the Synthetic Minority Over-sampling Technique (SMOTE), which has been successfully used in several biomedical studies [66]–[73]. Note, only the training set is oversampling (the test set contains real data only).

3.5 Classification

Several simple, yet powerful, classifiers are considered in this study. First, Fishers Linear Discriminant Analysis (FLDA) algorithm is utilised to determine the presence of linearity in the CTU-UHB dataset. A linear combination of features is adopted to find the direction along which the two classes are best separated. Data is projected onto a line in such a way that it maximises the distance between the means of the two classes while minimizing the variance within each class. Classification is performed in this one-dimensional space.

Ensemble classifiers have shown to have powerful classification and regression capabilities. In this study, we consider the Random Forest (RF) classifier [23], [74]. This algorithm uses an ensemble of many randomised decision-trees to vote on the classification outcome. Each decision-tree is randomised using a bootstrap statistical resampling technique, with random feature selection. The optimal split is calculated using different feature sets, which continues until the tree is fully grown without pruning. This procedure is repeated for all trees in the forest using different bootstrap samples of the data. Classifying new samples can then be achieved using a majority vote.

Finally, a Support Vector Machine is considered, which has previously been used to solve practical classification problems, particularly in biomedical domains [22], [75]–[77]. SVM binary classifiers maximise the margins in a hyperplane in such a way that it increases the distance between classes. In order to separate binary classes the SVM creates a linear separating hyperplane. The SVM achieves this by maximizing the margin between observations in this higher dimensional space.

3.6 Validation Methods

Holdout and k-Fold Cross-Validation are adopted as data splitting methods. In the Holdout approach an 80/20 split is adopted (80% for training and 20% for testing). The training and test sets contain randomly selected records from the CTG-UHB dataset. Since the exact selection of instances is random, the learning and test stages are repeated (oversampling on

the training set occurs within this process). The performance metrics for each model is averaged over 30 epochs. Under the k-fold method, five folds with one and 30 epoch configurations are used. Both methods are compared to validate the suitability of an 80/20 split. *Sensitivity* and *specificity* measures are adopted to evaluate the performance of binary classification tests. *Sensitivities* refer to the true positive rate for caesarean section deliveries, while, *specificities* measure the true negative rate for normal vaginal deliveries.

The *Area Under the Curve* (AUC) is used to evaluate [78] model performance in binary classification tasks [79]. While, Mean Squared Error (MSE) measures the differences between actual and predicted values for all data points. A MSE value of zero indicates that the model correctly classifies all instances. For miss-classifications, the MSE will be progressively larger.

4. RESULTS

This section presents the results for classifying caesarean section and vaginal delivery types using features extracted from the FHR signals contained in the CTG-UHB dataset. The feature set is split using an 80% holdout technique and 5-fold cross-validation. The performance metrics consist of *Sensitivity*, *Specificity*, *AUC*, and *MSE* values and are substantiated using 95% confidence intervals (95% CI). The initial evaluation provides a baseline for comparison with all subsequent evaluations considered in this study.

4.1 Using all Features from Original Data

In the first evaluation, all 13 FHR features extracted from the original data are utilised to train the classifiers. The average performance of each classifier is evaluated using 30 simulations.

4.1.1 Classifier Performance

The results in Table 4 show that the *Sensitivities* (caesarean section deliveries) for all classifiers are very low, while corresponding *Specificities* are high. This is expected, given that the dataset is skewed in favour of vaginal delivery records. 95% CI adjusted for *Sensitivity*, *Specificity*, *AUC* and *MSE* are determined using the FLDA, RF and SVM classification models.

Table 4: Classification Performance Metrics Using all Features from Original Data

Classifier	Sensitivity (95% CI)	Specificity (95% CI)	AUC (95% CI)	MSE (95% CI)
FLDA	0.02(0.01,0.03)	0.99(0.99,0.99)	0.68(0.65, 0.69)	0.08(0.07,0.08)
RF	0.02(0.00,0.04)	0.99(0.99,0.99)	0.71(0.68,0.73)	0.08(0.07, 0.08)
SVM	0.00(0.00,0.00)	0.99(0.99,0.99)	0.60(0.58,0.61)	0.08(0.07,0.08)

The *AUC* value for the SVM is relatively low, which equates to slightly better than chance, while the FLDA produces a slightly higher value and the RF classifier slightly higher again as shown in Table 4 and illustrated in Figure 3.

Performance Measures for all Features and Original Data

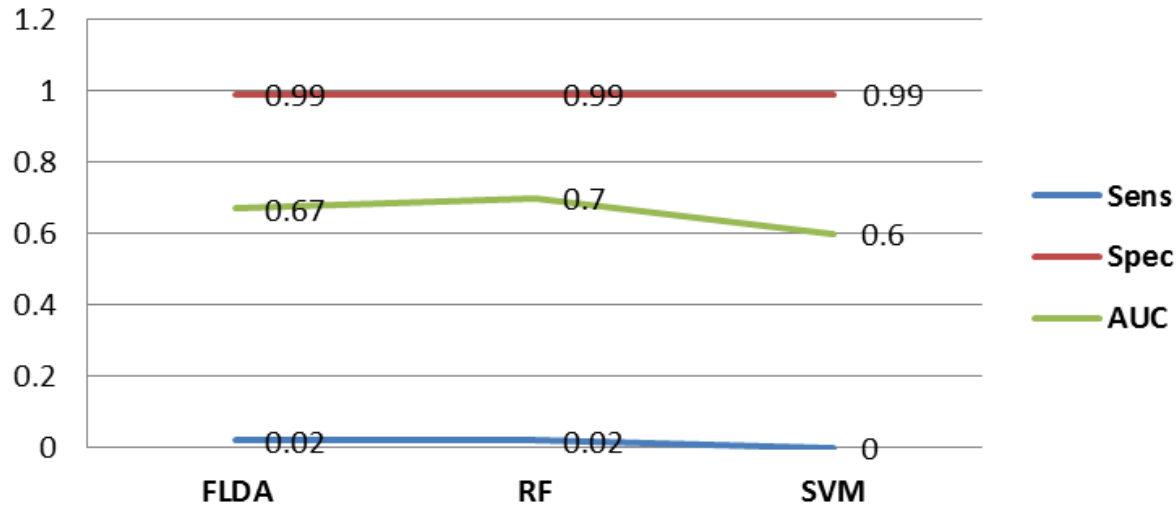


Figure 3: Sensitivity, Specificity and AUC Performance Measures for all Features and Original Data Using the FLDA, RF and SVM Classifiers

Table 5 shows the error rates – see Figure 4 for visual comparison. The errors are more or less consistent with the expected *MSE* base-rate of 8.3% (46 caesarean section deliveries/552 CTG FHR records). While 5-fold cross-validation does improve the error rates in the case of the SVM, the results are not considered statistically significant.

Table 5: Cross-Validation Error Rates for Original Data Using the FLDA, RF and SVM Classifiers

Classifier	Cross-Val 5-Fold 1-Rep	Cross-Val 5-Fold 30-Rep
	Error	Error
FLDA	0.09	0.09
RF	0.08	0.08
SVM	0.07	0.07

The primary reason *Sensitivities* are so low is that there are only 46 caesarean section records to model the class versus 506 normal vaginal delivery records. Conversely, *Specificities* are high because it is easier to classify normal vaginal deliveries due to better representation in the classifier models. As such, caesarean section cases need to be oversampled to normally distribute the data [80].

Cross-Validation for all Features and Original Data

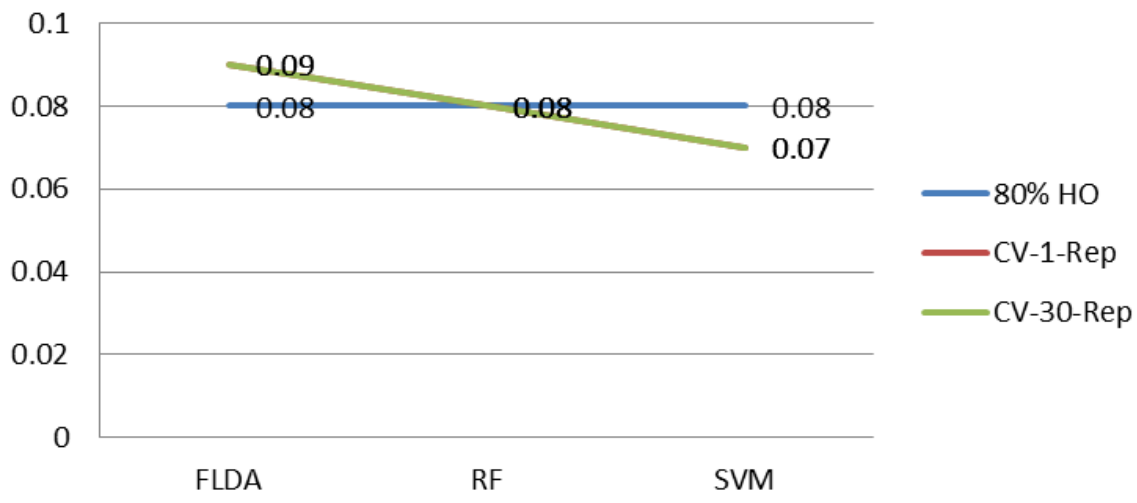


Figure 4: Cross-Validation Error Rates for all Features and Original Data Using the FLDA, RF and SVM Classifiers

4.2 Using all Features from SMOTE Data

Using the holdout technique the 80% allocated for training is resampled using the SMOTE algorithm (the remaining 20% is retained as real test data) by under sampling the majority by 100% and oversampling the minority by 600%. The classifiers are remodelled again using all 13 features and the average performance of each classifier is evaluated using 30 simulations.

4.2.1 Classifier Performance

The results, using the new SMOTEd training data (192 caesarean section records and 224 normal delivery records) and the real test data, can be found in Table 6 and illustrated in Figure 5.

Table 6: Classification Performance Metrics Using all Features from SMOTE Data

Classifier	Sensitivity (95% CI)	Specificity (95% CI)	AUC (95% CI)	MSE (95% CI)
FLDA	0.53(0.46,0.59)	0.70(0.68,0.72)	0.67(0.64,0.71)	0.08(0.07,0.08)
RF	0.59(0.54,0.65)	0.57(0.55,0.59)	0.62(0.60,0.64)	0.08(0.08,0.08)
SVM	0.66(0.58,0.74)	0.41(0.35,0.46)	0.55(0.52,0.57)	0.08(0.08,0.08)

These indicate that the *Sensitivities*, for all models have significantly improved. This is however at the expense of lower *Specificities*. Interestingly, the AUC values for all classifiers have decreased with the FLDA decreasing by one percent, the RF by nine percent and the SVM by five percent. Given that the *Sensitivity* and *Specificity* values are now more evenly distributed than the previous evaluation this is a much more accurate assessment of the AUC values.

Performance Measures for all Features and SMOTEd Data

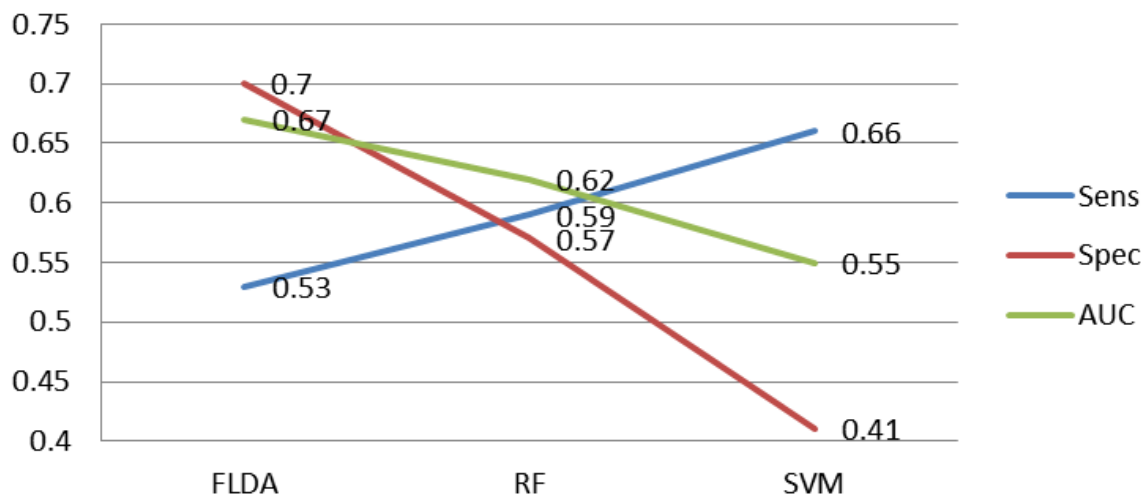


Figure 5: Sensitivity, Specificity and AUC Performance Measures for all Features and SMOTEd Data Using the FLDA, RF and SVM Classifiers

Table 7 and Figure 6 show that the error rates are more or less consistent with the previous set of results.

Table 7: Cross-Validation Error Rates for SMOTE Data Using the FLDA, RF and SVM Classifiers

Classifier	Cross-Val 5-Fold 1-Rep		Cross-Val 5-Fold 30-Rep	
	Error		Error	
FLDA	0.09		0.09	
RF	0.07		0.08	
SVM	0.05		0.05	

5-fold cross-validation does provide improvements over the holdout technique in some cases, however these are not considered statistically significant with the exception of the SVM.

Cross-Validation for all Features and SMOTEd Data

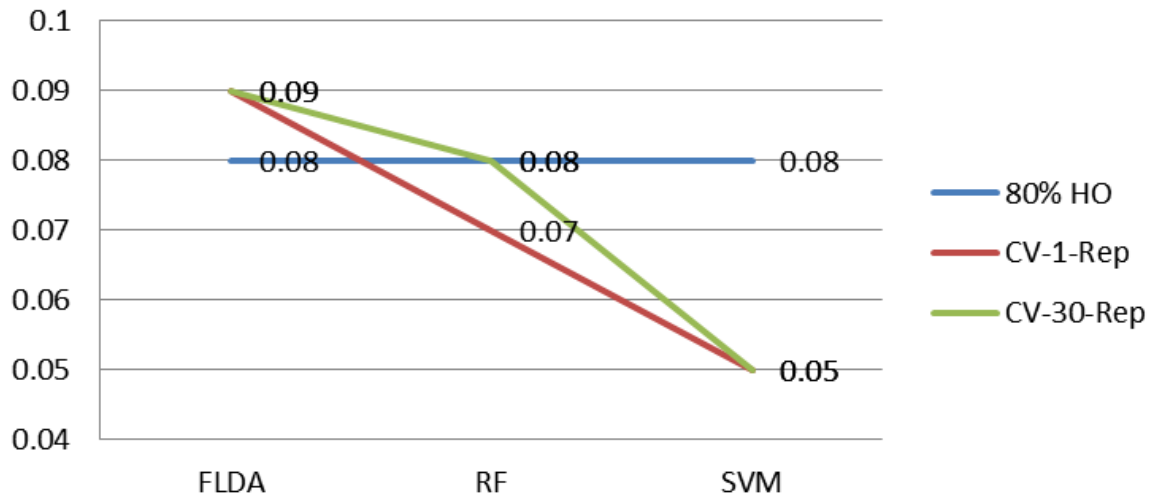


Figure 6: Cross-Validation Error Rates for all Features and SMOTEd Data Using the FLDA, RF and SVM Classifiers

4.3 Using RFE Selected Features from SMOTE Data

The eight RFE ranked features (DFA, RMS, FD, SD1, SDRatio, SD2, SampEn and STV) are used to remodel the classifiers and determine whether the previous results can be improved.

4.3.1 Classifier Performance

Looking at Table 8, there are some interesting results. The *Sensitivity* values remained roughly the same with the exception of the SVM which improved by 26%. The *Specificity* values have also improved slightly except the SVM. There were also notable improvements in the AUC values.

Table 8: Classification Performance Metrics Using RFE Selected Features from SMOTE Data

Classifier	Sensitivity (95% CI)	Specificity (95% CI)	AUC (95% CI)	MSE (95% CI)
FLDA	0.59(0.53,0.63)	0.71(0.69,0.72)	0.68(0.66,0.71)	0.08(0.07,0.08)
RF	0.76(0.70,0.81)	0.56(0.54,0.58)	0.70(0.68,0.73)	0.08(0.07,0.08)
SVM	0.52(0.45,0.59)	0.67(0.65,0.69)	0.63(0.59,0.66)	0.08(0.08,0.08)

While the RF produced the best *Sensitivity* values, its *Specificity* value is much lower than in the previous evaluation.

Performance Measures for RFE Features from SMOTEd Data

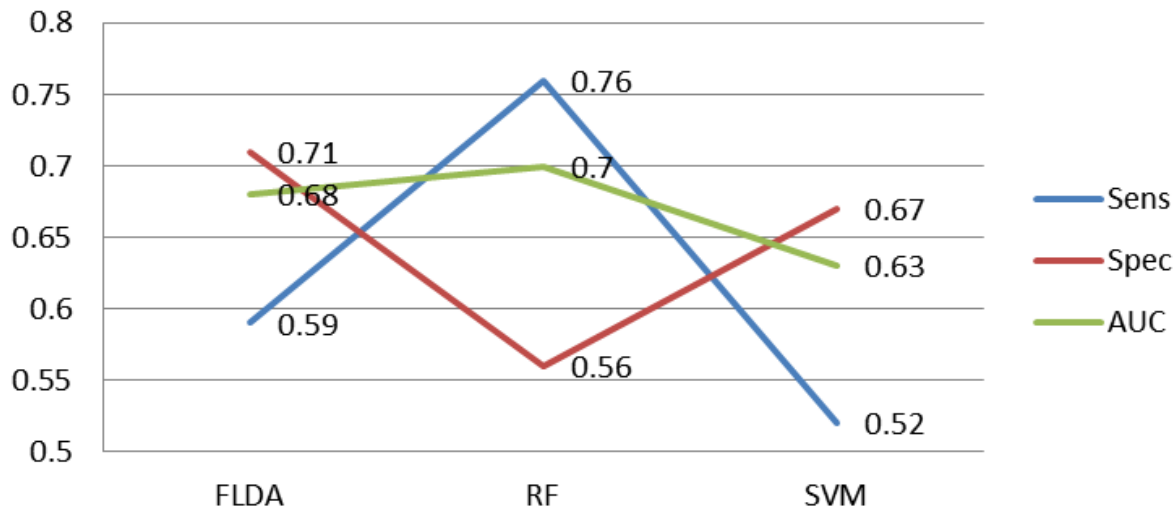


Figure 7: Sensitivity, Specificity and AUC Performance Measures for RFE Features from SMOTEd Data Using the FLDA, RF and SVM Classifiers

The *MSE* values, in Table 9 and illustrated in Figure 8, remained more or less the same.

Table 9: Cross-Validation Error Rates for SMOTE Data Using the FLDA, RF and SVM Classifiers

Classifier	Cross-Val 5-Fold 1-Rep		Cross-Val 5-Fold 30-Rep	
	Error	Error	Error	Error
FLDA	0.09		0.09	
RF	0.08		0.08	
SVM	0.05		0.05	

5-fold cross validation did not report any significant improvements on the *MSE* values previously reported and did not outperform those produced using the holdout technique.

Cross-Validation for all RFE Features from SMOTEd Data

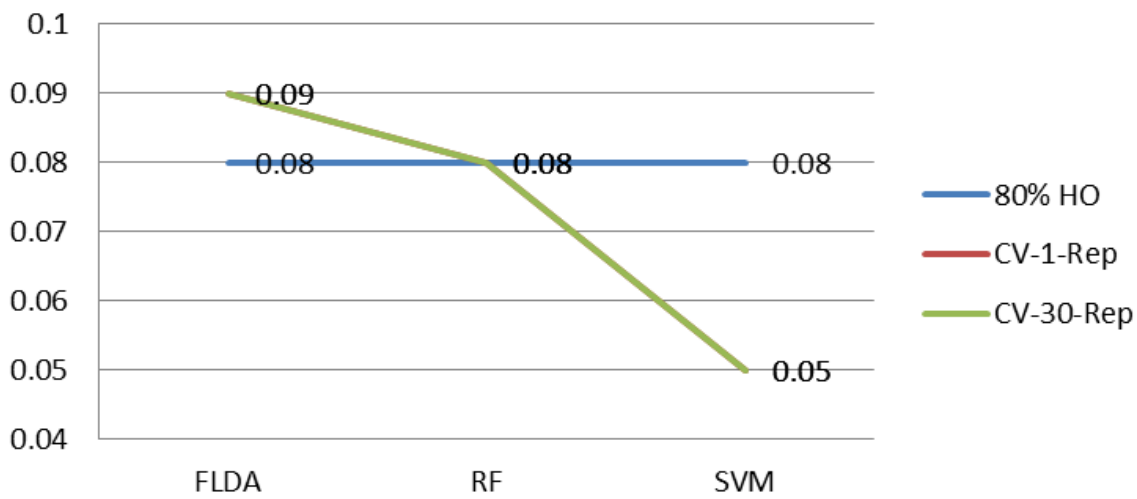


Figure 8: Cross-validation Error Rates for RFE Features and SMOTEd Data Using the FLDA, RF and SVM Classifiers

4.4 Using RFE Selected Features from SMOTE Data and Ensemble Modelling

The previous results indicate slight improvements using oversampling. The best model fit is achieved using the RF classifier with the RFE selected features from SMOTEd data, with 76% (95% CI: 70%,81%) for *Sensitivity*, 56% (95% CI: 54%,58%) for *Specificity*, 70% (95% CI: 68%,73%) for the *AUC*, with a 8% (95% CI: 7%,8%) *MSE*. In an attempt to improve the results, the next evaluation considers an ensemble model comprising FLDA, RF and SVM combinations.

4.4.1 Model Correlation Analysis

Model correlation analysis is performed and models with correlations less than 0.75 between predictions are retained and combined to form an ensemble classifier. Low correlation means that the models have good predictive capabilities, but in different ways. Correlations that are high, suggest that models are making the same or very similar predictions and this reduces the benefits of combining predictions. Consequently, the goal is to create a new classifier that utilises the strengths of each model to improve the overall metric values. Table 10 shows that the three models used in this study are below the 0.75 correlation threshold and are thus suitable candidates for ensemble modelling.

Table 10: Model Correlation Analysis for the FLDA, RF and SVM Classifiers

	FLDA	RF	SVM
FLDA	1.0000	0.6781	0.3741
RF	0.6781	1.0000	0.4703
SVM	0.3741	0.4703	1.0000

4.4.2 Classifier Performance

Table 11, presents the results for the different ensemble model combinations. The values for all performance metrics when using the ensemble classifier combinations have improved.

Table 11: Ensemble Classification Performance Metrics Using Classifier Ensemble Combinations

Ensemble	Sensitivity (95% CI)	Specificity (95% CI)	AUC (95% CI)	MSE (95% CI)
FLDA_RF_SVM	0.87(0.86,0.88)	0.90(0.89,0.91)	0.96(0.96,0.97)	0.09(0.09,0.10)
FLDA_RF	0.81(0.78,0.85)	0.90(0.87,0.94)	0.96(0.94,0.97)	0.08(0.05,0.11)
FLDA_SVM	0.71(0.68,0.73)	0.82(0.80,0.85)	0.87(0.86,0.88)	0.18(0.17,0.19)
RF_SVM	0.87(0.85,0.88)	0.91(0.89,0.92)	0.96(0.96,0.97)	0.08(0.07,0.09)

The best results were obtained from a FLDA, RF and SVM ensemble model with 87%(95% CI: 86%,88%) for Sensitivity, 90%(95% CI: 89%,91%) for Specificity, 96%(95% CI: 96%,97%) for the AUC with a 8%(95% CI: 9%,10%) MSE.

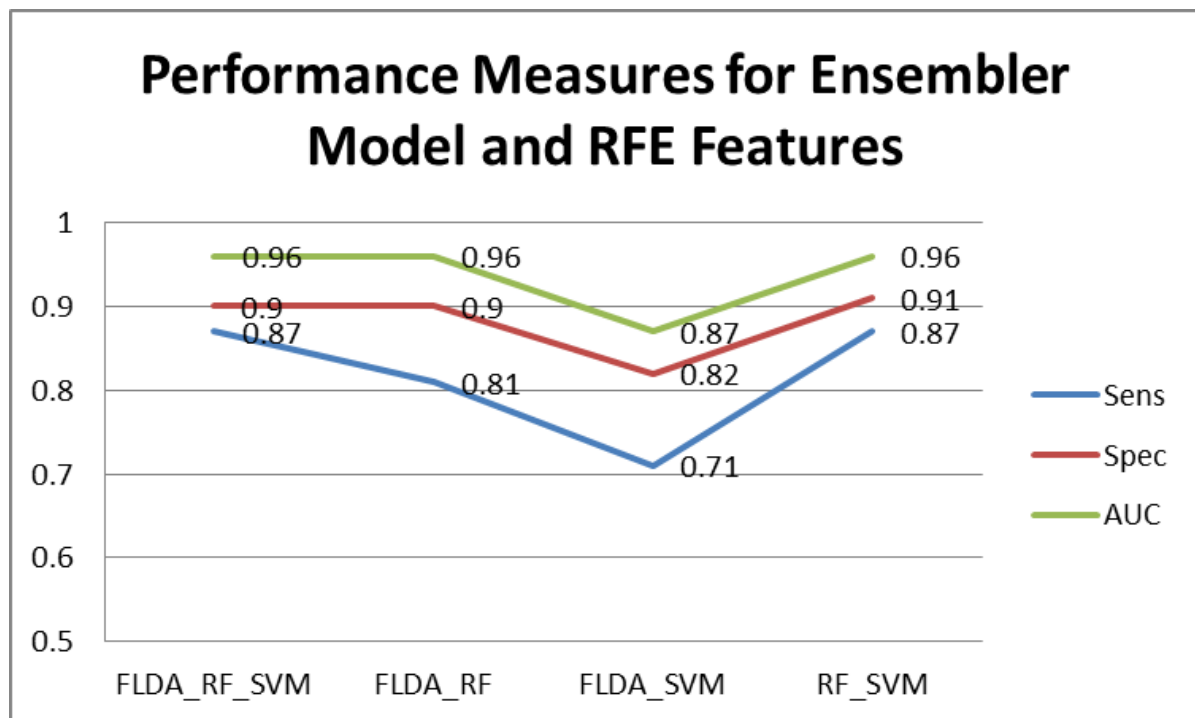


Figure 9: Sensitivity, Specificity and AUC Performance Measures for Ensembler Model and RFE Features from SMOTEd Data Using the FLDA, RF and SVM Classifiers

5. DISCUSSION

This study used machine learning to classify caesarean section and vaginal delivery types using CTG records from 552 subjects. The main objective was determine whether machine learning could be used to optimise the decisions made by obstetricians and midwives, in the presence of FHR traces, linked to caesarean section and normal vaginal deliveries. To

achieve this machine learning algorithms were modelled using the 552 records from the CTU-UHB database. No pre-selection of perinatal complications was made. In the pre-processing tasks, the FHR signal was filtered, and noise and low-quality artefacts were removed based on findings in previous studies [38], [39], [81]–[83].

Several features were extracted from the raw FHR signal. The resulting feature set was used to train FLDA, RF, and SVM classifiers. The initial classification results achieved high *Specificities* (normal deliveries). However, this was at the cost of very low *Sensitivities* (caesarean section deliveries) which in this study are considered more important. Cross-validation was utilised to increase the *Sensitivity* values. However, the MSE improvements were not statistically significant. This was attributed to the disproportionate number of vaginal and caesarean section delivery records and a skewed distribution towards the majority class. The minimum error rate displayed across all classifiers was approximately 8% using the holdout technique. Low *MSE* error rates are subjected to classifiers minimizing the probability of error when there is insufficient evidence to classify otherwise.

Using the SMOTE algorithm to oversample the training significantly improved the *Sensitivity* for all classifiers but reduced all *Specificities* when 13 features were used. We argue that while oversampling is not ideal, it is a recognised way to normally distribute datasets [66]–[72]. The *AUC* values across all classifiers did not improve. The *MSE* values remained broadly the same. The best results were achieved using the RF classifier with 59% (95% CI: 54%, 65%) for *Sensitivity*, 57% (95% CI: 55%, 59%) for *Specificity*, 62% (95% CI: 60%, 64%) for the *AUC*, with a 8% (95% CI: 8%, 8%) *MSE*. We considered the RF classifier to be the best as indicated by the approximate balance between *Sensitivity* and *Specificity* values. However, the results are not sufficient for use in a medical decision support system.

Using the RFE algorithm, five features were considered to have no or very low discriminative capacity and were removed. This left eight features for further classifier modelling and evaluation. The results showed improvements in all classifiers with the best results obtained from the RF model with 76% (95% CI: 70%, 81%) for *Sensitivity*, 56% (95% CI: 54%, 58%) for *Specificity*, 70% (95% CI: 68%, 73%) for the *AUC*, with a 8% (95% CI: 7%, 8%) *MSE*.

Combining the classifiers into ensemble models demonstrated a marked improvement in all of the classifier models. The best results were obtained when the FLDA, RF and SVM classifiers were combined with overall values of 87% (95% CI: 86%, 88%) for *Sensitivity*, 90% (95% CI: 89%, 91%) for *Specificity*, 96% (95% CI: 96%, 97%) for the *AUC*, with a 8% (95% CI: 9%, 10%) *MSE*. Ensemble modelling is able to achieve this by running the individual models and synthesising the results to improve the overall accuracy. In the case of the SVM, it has good generalisation capabilities and in this study, the eight features were used to maximise the margins in the hyperplane to increase the distance between classes to provide better discrimination. In the case of the RF, each decision-tree is randomised using a bootstrap statistical resampling technique, with random feature selection. Many randomised decision-trees use the data points of a particular class to vote and classify new data points. This is particularly useful for observations located close to the decision boundary, where classifiers such as the SVM, based on isolated data points, find them difficult to classify. In the context of linear discrimination, the results show that using the FLDA it is not possible to maximise the between class variance sufficiently to remove class overlap. This shows that classification errors are unavoidable around the decision boundary. In a similar way to the SVM, the FLDA finds it easier to classify observations farthest away from the decision boundary than those close to it or overlapping using the CTU-UHB dataset.

Consequently, it is clear to see that through ensemble modelling, the strengths of each model can be utilised to distinguish between caesarean section and vaginal delivery types using the FHR signal. In particular, the results demonstrate that the ensemble model, trained using the DFA, RMS, FD, SD1, SDRatio, SD2, SampEn, and STV, features, provides significant improvements, using a robust methodology, on many previously reported machine learning studies in automated Cardiotocography trace interpretation [16], [45], [52], [53], [75], [84], [85].

6. CONCLUSIONS AND FUTURE WORK

Complications during labour can result in adverse perinatal outcomes and in severe cases death. Consequently, early detection and the prediction of pathological outcomes could help to reduce foetal morbidity and mortality rates worldwide and indicate if surgical intervention, such as caesarean section, is required. Human CTG analysis is used to monitor the foetus during labour. However, poor human interpretation has led to high inter and intra observer variability. A strong body of evidence has therefore suggested that automated computer analysis of CTG signals might provide a viable way of diagnosing true perinatal complications and predict the early onset of pathological outcomes with much less variability and better accuracy.

The study presented in this paper explored this idea and utilised FHR signals from CTG traces and supervised machine learning, to train and classify caesarean section and vaginal deliveries. This was achieved using an ensemble classifier modelled using oversampled training data consisting of eight RFE ranked features. The results demonstrate using an ensemble model consisting of a FLDA, RF, and SVM model, it is possible to obtain 87% (95% CI: 86%, 88%) for *Sensitivity*, 90% (95% CI: 89%, 91%) for *Specificity*, and 96% (95% CI: 96%, 97%) for *AUC*, with a 9% (95% CI: 9%, 10%) *MSE*.

While, the results are encouraging, further more in-depth studies are required. For example, mapping signals to pH values or a range of values for multivariate classification would be interesting. This would provide a granular assessment of outcomes potentially more accurate and inclusive than simply predicting whether a mother will have a caesarean section or vaginal delivery. Future research will also explore opportunities to obtain a much larger normally distribution dataset, removing the need for oversampling.

We only considered the FHR signal in this study, because it provides direct information about the foetus's state. However, it would be useful to create an extended dataset that encompasses features extracted from the UC signal. Studying the effects UC has on the foetus during pregnancy provides valuable information as can be seen in our previous work [83], and could yield additional important information. Lastly, it would be interesting to remove the feature engineering stage altogether in favour of deep learning and stacked autoencoders. This would force models to learn meaning for information or structure in the data that could potentially be more representative of the data than the features considered in this paper.

Overall, the study demonstrates that classification algorithms provide an interesting line of enquiry worth exploring, when classifying caesarean section and vaginal delivery types.

REFERENCES

- [1] J. B. Warren, W. E. Lambert, R. Fu, J. M. Anderson, and A. B. Edelman, “Global neonatal and perinatal mortality: a review and case study for the Loreto Province of Peru,” *Res. Reports Neonatol.*, vol. 2, pp. 103–113, 2012.
- [2] R. Brown, J. H. B. Wijekoon, A. Fernando, E. D. Johnstone, and A. E. P. Heazell, “Continuous objective recording of fetal heart rate and fetal movements could reliably identify fetal compromise, which could reduce stillbirth rates by facilitating timely management,” *Med. Hypotheses*, vol. 83, no. 3, pp. 410–417, 2014.
- [3] S. Rees and T. Inder, “Fetal and neonatal origins of altered brain development,” *Early Hum. Dev.*, vol. 81, no. 9, pp. 753–761, 2005.
- [4] S. Rees, R. Harding, and D. Walker, “An adverse intrauterine environment: implications for injury and altered development of the brain,” *Int. J. Dev. Neurosci.*, vol. 26, no. 1, pp. 3–11, 2008.
- [5] B. Chudacek, J. Spilka, M. Bursa, P. Janku, L. Hruban, M. Huptych, and L. Lhotska, “Open access intrapartum CTG database,” *BMC Pregnancy Childbirth*, vol. 14, no. 16, pp. 1–12, 2014.
- [6] G. Bogdanovic, A. Babovic, M. Rizvanovic, D. Ljuca, G. Grgic, and J. Djuranovic-Milicic, “Cardiotocography in the Prognosis of Perinatal Outcome,” *Med. Arch.*, vol. 68, no. 2, pp. 102–105, 2014.
- [7] J. Kessler, D. Moster, and S. Albrechfsen, “Delay in intervention increases neonatal morbidity in births monitored with Cardiotocography and ST-waveform analysis,” *Acta Obs. Gynecol Scand*, vol. 93, no. 2, pp. 175–81, 2014.
- [8] J. Hasegawa, A. Sekizawa, T. Ikeda, M. Koresawa, S. Ishiwata, M. Kawabata, and K. Kinoshita, “Clinical Risk Factors for Poor Neonatal Outcomes in Umbilical Cord Prolapse,” *J. Matern. Neonatal Med.*, vol. 29, no. 10, pp. 1652–1656, 2016.
- [9] S. Kundu, E. Kuehnle, C. Schippert, J. von Ehr, P. Hillemanns, and I. Staboulidou, “Estimation of neonatal outcome artery pH value according to CTG interpretation of the last 60 min before delivery: a retrospective study. Can the outcome pH value be predicted?,” *Arch. Gynecol. Obstet.*, vol. 296, no. 5, pp. 897–905, 2017.
- [10] C. Garabedian, L. Butruille, E. Drumez, E. S. Servan Schreiber, S. Bartolo, G. Bleu, V. Mesdag, P. Deruelle, J. De Jonckheere, and V. Houfflin-Debarge, “Inter-observer reliability of 4 fetal heart rate classifications,” *J. Gynecol. Obstet. Hum. Reprod.*, vol. 46, no. 2, pp. 131–135, 2017.
- [11] S. Kundu, E. Kuehnle, C. Schippert, J. von Ehr, P. Hillemanns, and I. Staboulidou, “Estimation of neonatal outcome artery pH value according to CTG interpretation of the last 60 min before delivery: a retrospective study. Can the outcome pH value be predicted?,” *Arch. Gynecol. Obstet.*, vol. 296, no. 5, pp. 897–905, 2017.
- [12] P. A. Warrick, E. F. Hamilton, D. Precup, and R. E. Kearney, “Classification of normal and hypoxic fetuses from systems modeling of intrapartum Cardiotocography,” *IEEE Trans. Biomed. Eng.*, vol. 57, no. 4, pp. 771–779, 2010.

- [13] J. Spilka, G. Georgoulas, P. Karvelis, and V. Chudacek, “Discriminating Normal from ‘Abnormal’ Pregnancy Cases Using an Automated FHR Evaluation Method,” *Artif. Intell. Methods Appl.*, vol. 8445, pp. 521–531, 2014.
- [14] M. Romano, P. Bifulco, M. Ruffo, G. Improta, F. Clemente, and M. Cesarelli, “Software for computerised analysis of cardiotocographic traces,” *Comput. Methods Programs Biomed.*, vol. 124, pp. 121–137, 2016.
- [15] A. Pinas and E. Chadrarahan, “Continuous Cardiotocography During Labour: Analysis, Classification and Management.,” *Best Pract. Res. Clin. Obstet. Gynaecol.*, vol. 30, pp. 33–47, 2016.
- [16] P. A. Warrick, E. F. Hamilton, D. Precup, and R. E. Kearney, “Classification of Normal and Hypoxic Fetuses From Systems Modeling of Intrapartum Cardiotocography,” *IEEE Trans. Biomed. Eng.*, vol. 57, no. 4, pp. 771–779, 2010.
- [17] H. Sahin and A. Subasi, “Classification of the cardiotocogram data for anticipation of fetal risks using machine learning techniques,” *Appl. Soft Comput.*, vol. 33, pp. 231–238, 2015.
- [18] H. Ocak and H. M. Ertunc, “Prediction of fetal state from the cardiotocogram recordings using adaptive neuro-fuzzy inference systems,” *Neural Comput. Applications*, vol. 22, no. 6, pp. 1583–1589, 2013.
- [19] C. Rotariu, A. Pasarica, G. Andruseac, H. Costin, and D. Nemescu, “Automatic analysis of the fetal heart rate variability and uterine contractions,” in *IEEE Electrical and Power Engineering*, 2014, pp. 553–556.
- [20] C. Rotariu, A. Pasarica, H. Costin, and D. Nemescu, “Spectral analysis of fetal heart rate variability associated with fetal acidosis and base deficit values,” in *International Conference on Development and Application Systems*, 2014, pp. 210–213.
- [21] K. Maeda, “Modalities of fetal evaluation to detect fetal compromise prior to the development of significant neurological damage,” *J. Obstet. adn Gynaecol. Res.*, vol. 40, no. 10, pp. 2089–2094, 2014.
- [22] H. Ocak, “A Medical Decision Support System Based on Support Vector Machines and the Genetic Algorithm for the Evaluation of Fetal Well-Being,” *J. Med. Syst.*, vol. 37, no. 2, p. 9913, 2013.
- [23] T. Peterek, P. Gajdos, P. Dohnalek, and J. Krohova, “Human Fetus Health Classification on Cardiotocographic Data Using Random Forests,” in *Intelligent Data Analysis and its Applications*, 2014, pp. 189–198.
- [24] R. M. Grivell, Z. Alfirevic, G. M. L. Gyte, and D. Devane, “Cardiotocography (a form of electronic fetal monitoring) for assessing a baby’s well-being in the womb during pregnancy,” *Syst. Rev.*, vol. 2015, no. 9, 2015.
- [25] A. R. Webb and K. D. Copsey, *Statistical Pattern Recognition*. 2011, pp. 1–642.
- [26] V. S. Talaulikar, V. Lowe, and S. Arulkumaran, “Intrapartum fetal surveillance.,” *Obstet. Gynaecol. Reprod. Med.*, vol. 24, no. 2, pp. 45–55, 2014.

- [27] A. L. Goldberger, L. A. N. Amaral, L. Glass, J. M. Hausdorff, and E. Al., “PhysioBank, PhysioToolkit, and PhysioNet: Components of a new research resource for complex physiologic signals.”
- [28] R. Mantel, H. P. van Geijn, F. J. Caron, J. M. Swartjies, van W. E. E., and H. W. Jongasma, “Computer analysis of antepartum fetal heart rate: 2. Detection of accelerations and decelerations,” *Int. J. Biomed Comput.*, vol. 25, no. 4, pp. 273–286, 1990.
- [29] H. M. Franzcog, “Antenatal foetal heart monitoring,” *Best Pract. Res. Clin. Obstet. Gynaecol.*, vol. 38, pp. 2–11, 2017.
- [30] J. Camm, “Heart rate variability: standards of measurement, physiological interpretation and clinical use. Task Force of the European Society of Cardiology and the North American Society of Pacing and Electrophysiology,” *Circulation*, vol. 93, no. 5, pp. 1043–65, 1996.
- [31] L. Stroux, C. W. Redman, A. Georgieva, S. J. Payne, and G. D. Clifford, “Doppler-based fetal heart rate analysis markers for the detection of early intrauterine growth restriction,” *Acta Obstet. Gynecol. Scand.*, vol. 96, no. 11, pp. 1322–1329, 2017.
- [32] M. Romano, L. Iuppariello, A. M. Ponsiglione, G. Imrota, P. Bifulco, and M. Cesarelli, “Frequency and Time Domain Analysis of Foetal Heart Rate Variability with Traditional Indexes: A Critical Survey,” *Comput. Math. Methods Med.*, vol. 2016, no. 9585431, pp. 1–12, 2016.
- [33] C. Buhimschi, M. B. Boyle, G. R. Saade, and R. E. Garfield, “Uterine activity during pregnancy and labor assessed by simultaneous recordings from the myometrium and abdominal surface in the rat.,” *Am. J. Obstet. Gynecol.*, vol. 178, no. 4, pp. 811–22, Apr. 1998.
- [34] C. Buhimschi, M. B. Boyle, and R. E. Garfield, “Electrical activity of the human uterus during pregnancy as recorded from the abdominal surface,” *Obstet. Gynecol.*, vol. 90, no. 1, pp. 102–111, 1997.
- [35] C. Buhimschi and R. E. Garfield, “Uterine contractility as assessed by abdominal surface recording of electromyographic activity in rats during pregnancy.,” *Am. J. Obstet. Gynecol.*, vol. 174, no. 2, pp. 744–53, Feb. 1996.
- [36] J. S. Richman and J. R. Moorman, “Physiological time-series analysis using approximate entropy and sample entropy,” *Am. J. Physiol. - Hear. Circ. Physiol.*, vol. 278: H2039, no. 6, 2000.
- [37] M. G. Signorini, A. Fanelli, and G. Magenes, “Monitoring fetal heart rate during pregnancy: contributions from advanced signal processing and wearable technology,” *Comput. Math. Methods Med.*, vol. 2014, no. 707581, pp. 1–10, 2014.
- [38] M. Romano, M. Cesarelli, P. Bifulco, M. Ruffo, A. Frantini, and G. Pasquariello, “Time-frequency analysis of CTG signals,” *Curr. Dev. Theory Appl. Wavelets*, vol. 3, no. 2, pp. 169–192, 2009.

- [39] M. J. Rooijakers, S. Song, C. Rabotti, G. Oei, J. W. M. Bergmans, E. Cantatore, and M. Mischi, “Influence of Electrode Placement on Signal Quality for Ambulatory Pregnancy Monitoring,” *Comput. Math. Methods Med.*, vol. 2014, no. 2014, pp. 1–12, 2014.
- [40] M. G. Signorini, G. Magenes, S. Cerutti, and D. Arduini, “Linear and nonlinear parameters for the analysis of fetal heart rate signal from cardiotocographic recordings,” *IEEE Trans. Biomed. Eng.*, vol. 50, no. 3, pp. 365–374, 2003.
- [41] S. Siira, T. Ojala, E. Ekholm, T. Vahlberg, S. Blad, and K. G. Rosen, “Change in heart rate variability in relation to a significant ST-event associates with newborn metabolic acidosis,” *BJOG An Int. J. Obstet. Gynaecol.*, vol. 114, no. 7, pp. 819–823, 2007.
- [42] V. J. Laar, M. M. Porath, C. H. L. Peters, and S. G. Oei, “Spectral analysis of fetal heart rate variability for fetal surveillance: review of the literature,” *Acta Obs. Gynecol Scand*, vol. 87, no. 3, pp. 300–306, 2008.
- [43] P. Melillo, R. Izzo, A. Orrico, P. Scala, M. Attanasio, M. Mirra, N. De Luca, and L. Pecchia, “Automatic Prediction of Cardiovascular and Cerebrovascular Events Using Heart Rate Variability Analysis,” *PLoS One*, vol. 10, no. 3, p. e0118504, 2015.
- [44] H. Goncalves, D. Ayres-de-Campos, and J. Bernardes, “Linear and Nonlinear Analysis of Fetal Heart Rate Variability. In Fetal Development,” in *Fetal Development*, 2016, pp. 119–132.
- [45] J. Spilka, V. Chudacek, M. Koucky, L. Lhotska, M. Huptych, P. Janku, G. Georgoulas, and C. Stylios, “Using nonlinear features for fetal heart rate classification,” *Biomed. Signal Process. Control*, vol. 7, no. 4, pp. 350–357, 2012.
- [46] J. Spilka, V. Chudacek, M. Koucky, and L. Lhotska, “Assessment of non-linear features for intrapartal fetal heart rate classification,” in *The 9th International Conference on Information Technology and Applications in Biomedicine*, 2009, pp. 1–4.
- [47] P. Hopkins, N. Outram, N. Lofgren, E. C. Ifeachor, and K. G. Rosen, “A Comparative Study of Fetal Heart Rate Variability Analysis Techniques,” in *The 28th IEEE Annual International Conference on Engineering in Medicine and Biology Society.*, 2006, pp. 1784–1787.
- [48] P. Abry, S. G. Roux, V. Chudacek, P. Borgnat, P. Goncalves, and M. Doret, “Hurst Exponent and IntraPartum Fetal Heart Rate: Impact of Decelerations,” in *26th IEEE International Symposium on Computer-Based Medical Systems*, 2013, pp. 131–136.
- [49] M. Haritopoulos, A. Illanes, and A. K. Nandi, “Survey on Cardiotocography Feature Extraction Algorithms for Foetal Welfare Assessment,” in *Springer Mediterranean Conference on Medical and Biological Engineering and Computing*, 2016, pp. 1187–1192.
- [50] G. Koop, M. H. Pesaran, and S. M. Potter, “Impulse response analysis in nonlinear multivariate models,” *J. Econom.*, vol. 74, no. 1, pp. 119–147, 1996.

- [51] E. Blinx, K. G. Brurberg, E. Reierth, L. M. Rein, and P. Oian, “ST waveform analysis versus Cardiotocography alone for intrapartum fetal monitoring: a systematic review and meta-analysis of randomized trials,” *Acta Obstet. Gynancelogica Scand.*, vol. 95, no. 1, pp. 16–27, 2016.
- [52] H. Ocak, “A Medical Decision Support System Based on Support Vector Machines and the Genetic Algorithm for the Evaluation of Fetal Well-Being,” *Springer J. Med. Syst.*, vol. 37, no. 9913, pp. 1–9, 2013.
- [53] E. Yilmaz and C. Kilikcier, “Determination of Fetal State from Cardiotocogram Using LS-SVM with Particle Swarm Optimization and Binary Decision Tree,” *Comput. Math. Methods Med.*, vol. 2013, no. 487179, pp. 1–8, 2013.
- [54] H. Ocak and H. M. Ertunc, “Prediction of fetal state from the cardiotocogram recordings using adaptive neuro-fuzzy inference systems,” *Neural Comput. Appl.*, vol. 23, no. 6, pp. 1583–1589, 2013.
- [55] M. E. Menai, F. J. Mohder, and F. Al-mutairi, “Influence of Feature Selection on Naïve Bayes Classifier for Recognizing Patterns in Cardiotocograms,” *J. Med. Bioeng.*, vol. 2, no. 1, pp. 66–70, 2013.
- [56] E. M. Karabulut and T. Ibrikci, “Analysis of Cardiotocogram Data for Fetal Distress Determination by Decision Tree Based Adaptive Boosting Approach,” *J. Comput. Commun.*, vol. 2, no. 9, pp. 32–37, 2014.
- [57] D. Rindskopf and W. Rindskopf, “The value of latent class analysis in medical diagnosis,” *Stat. Med.*, vol. 5, no. 1, pp. 21–27, 1986.
- [58] M. Romano, G. Faiella, P. Bifulco, D. Addio, F. Clemente, and M. Cesarelli, “Outliers Detection and Processing in CTG Monitoring,” in *Mediterranean Conference on Medical and Biological Engineering and Computing*, 2013, pp. 651–654.
- [59] P. A. Warrick, E. F. Hamilton, D. Precup, and R. E. Kearney, “Identification of the dynamic relationship between intra-partum uterine pressure and fetal heart rate for normal and hypoxic fetuses,” *IEEE Trans. Biomed. Eng.*, vol. 56, no. 6, pp. 1587–1597, 2009.
- [60] H. Goncalves, A. Costa, D. Ayres-de-Campos, C. Costa-Santos, A. P. Rocha, and J. Benardes, “Comparison of real beat-to-beat signals with commercially available 4 Hz sampling on the evaluation of foetal heart rate variability,” *Med. Biol. Eng. Comput.*, vol. 51, no. 6, 2013.
- [61] P. A. Warrick and E. F. Hamilton, “Subspace detection of the impulse response function from intrapartum uterine pressure and fetal heart rate variability,” in *IEEE Computing in Cardiology Conference*, 2013, pp. 85–88.
- [62] P. A. Warrick and E. F. Hamilton, “Discrimination of Normal and At-Risk Populations from Fetal Heart Rate Variability,” *Comput. Cardiol. (2010)*, vol. 41, pp. 1001–1004, 2014.

- [63] G. Improta, M. Romano, A. Ponsiglione, P. Bifulco, G. Faiella, and M. Cesarelli, “Computerized Cardiotocography: A Software to Generate Synthetic Signals,” *J Heal. Med Informat*, vol. 5, no. 4, pp. 1–6, 2014.
- [64] I. Nunes and D. Ayres-de-Campos, “Computer Analysis of Foetal Monitoring Systems,” *Best Pract. Res. Clin. Obstet. Gynaecol.*, vol. 30, pp. 68–78, 2016.
- [65] P. M. Granitto and A. B. Bohorquez, “Feature selection on wide multiclass problems using OVA-RFE,” *Intel. Artif.*, vol. 44, no. 2009, pp. 27–34, 2009.
- [66] L. M. Taft, R. S. Evans, C. r. Shyu, M. J. Egger, N. Chawla, J. A. Mitchell, S. N. Thornton, B. Bray, and M. Varner, “Countering imbalanced datasets to improve adverse drug event predictive models in labor and delivery,” *J. Biomed. Informatics2*, vol. 42, no. 2, pp. 356–364, 9AD.
- [67] T. Sun, R. Zhang, J. Wang, X. Li, and X. Guo, “Computer-Aided Diagnosis for Early-Stage Lung Cancer Based on Longitudinal and Balanced Data,” *PLoS One*, vol. 8, no. 5, p. e63559, 2013.
- [68] W. Lin and J. J. Chen, “Class-imbalanced classifiers for high-dimensional data,” *Brief. Bioinform.*, vol. 14, no. 1, pp. 13–26, 2013.
- [69] T. Sun, R. Zhang, J. Wang, X. Li, and X. Guo, “Computer-Aided Diagnosis for Early-Stage Lung Cancer Based on Longitudinal and Balanced Data,” *PLoS One*, vol. 8, no. 5, p. e63559, 2013.
- [70] J. Nahar, T. Imam, K. S. Tickle, A. B. M. Shawkat Ali, and Y. P. Chen, “Computational Intelligence for Microarray Data and Biomedical Image Analysis for the Early Diagnosis of Breast Cancer,” *Expert Syst. Appl.*, vol. 39, no. 16, pp. 12371–12377, 2012.
- [71] R. Blagus and L. Lusa, “SMOTE for High-Dimensional Class-Imbalanced Data,” *BMC Bioinformatics*, vol. 14, no. 106, 2013.
- [72] Y. Wang, M. Simon, P. Bonde, B. U. Harris, J. J. Teuteberg, R. L. Kormos, and J. F. Antaki, “Prognosis of Right Ventricular Failure in Patients with Left Ventricular Assist Device Based on Decision Tree with SMOTE,” *Trans. Inf. Technol. Biomed.*, vol. 16, no. 3, 2012.
- [73] N. V. Chawla, K. W. Bowyer, L. O. Hall, and W. P. Kegelmeyer, “SMOTE: Synthetic Minority Over-Sampling Technique,” *J. Artif. Intell. Res.*, vol. 16, no. 1, pp. 321–357, 2002.
- [74] P. Tomas, J. Krohova, P. Dohnalek, and P. Gajdos, “Classification of Cardiotocography records by random forest,” in *36th IEEE International Conference on Telecommunications and Signal Processing*, 2013, pp. 620–623.
- [75] N. Krupa, M. A. Ma, E. Zahedi, S. Ahmed, and F. M. Hassan, “Antepartum fetal heart rate feature extraction and classification using empirical mode decomposition and support vector machine,” *Biomed. Eng. Online*, vol. 10, no. 6, pp. 1–15, 2011.

- [76] G. Georgoulas, C. D. Stylios, and P. P. Groumpas, “Predicting the risk of metabolic acidosis for newborns based on fetal heart rate signal classification using support vector machines,” *IEEE Trans Biomed Eng*, vol. 53, no. 5, pp. 875–884, 2006.
- [77] B. Moslem, M. Khalil, and M. Diab, “Combining multiple support vector machines for boosting the classification accuracy of uterine EMG signals,” in *18th IEEE International Conference on Electronics, Circuits and Systems*, 2011, pp. 631–634.
- [78] T. Fawcett, “An Introduction to ROC analysis,” *Pattern Recognit. Lett.*, vol. 27, no. 8, pp. 861–874, 2006.
- [79] T. A. Lasko, J. G. Bhagwat, K. H. Zou, and L. Ohno-Machada, “The use of receiver operating characteristic curves in biomedical informatics,” *J. Biomed. Inform.*, vol. 38, no. 5, pp. 404–15, 2005.
- [80] L. Tong, Y. Change, and S. Lin, “Determining the optimal re-sampling strategy for a classification model with imbalanced data using design of experiments and response surface methodologies,” *Expert Syst. Appl.*, vol. 38, no. 4, pp. 4222–4227, 2011.
- [81] M. G. Signorini, G. Magenes, S. Cerutti, and D. Arduini, “Linear and nonlinear parameters for the analysis of fetal heart rate signal from cardiotocographic recordings,” *IEEE Trans Biomed Eng*, vol. 50, no. 3, pp. 365–74, 2003.
- [82] G. Fele-Žorž, G. Kavsek, Z. Novak-Antolic, and F. Jager, “A comparison of various linear and non-linear signal processing techniques to separate uterine EMG records of term and pre-term delivery groups,” *Med. Biol. Eng. Comput.*, vol. 46, no. 9, pp. 911–22, 2008.
- [83] P. Fergus, P. Cheung, P. Hussain, D. Al-Jumeily, C. Dobbins, and S. Iram, “Prediction of Preterm Deliveries from EHG Signals Using Machine Learning,” *PLoS One*, vol. 8, no. 10, p. e77154, 2013.
- [84] R. Czabanski, J. Jezewski, A. Matonia, and M. Jezewski, “Computerized analysis of fetal heart rate signals as the predictor of neonatal acidemia,” *Expert Syst. Appl.*, vol. 39, no. 15, pp. 11846–11860, 2012.
- [85] G. Georgoulas, C. Stylios, V. Chudecek, M. Macas, J. Bernardes, and L. Lhotska, “Classification of fetal heart rate signals based on features selected using the binary particle swarm algorithm,” in *World Congress on Medical Physics and Biomedical Engineering*, 2006, pp. 1156–1159.